Materials Science-Poland, 36(4), 2018, pp. 630-637
http://www.materialsscience.pwr.wroc.pl/
DOI: 10.2478/msp-2018-0094

Influence of L-threonine on the growth, structural, optical, mechanical and nonlinear optical properties of tartaric acid single crystal

G. THILAKAVATHI[1,2], R. ARUN KUMAR[1,3,*], V. GUNASEKARAN[4]

[1]G.R.D Center for Materials Research, PSG College of Technology, Coimbatore-641004, India
[2]Department of Physics, Dr. N.G.P. Institute of Technology, Coimbatore-641048, India
[3]Department of Physics, PSG College of Technology, Coimbatore-641004, India
[4]Department of Materials Science, Central University of Tamil Nadu, Thiruvarur-610 005, India

Single crystals of pure and L-threonine added tartaric acid (LT/TA), organic nonlinear optical (NLO) materials were grown from their respective aqueous solution by slow evaporation method. The crystalline nature of the grown crystals was confirmed by powder X-ray diffraction analysis (XRD). UV-Vis-NIR absorption and transmission spectra revealed that the lower cut-off wavelength was around 281 nm and the crystals exhibited high transmission over visible and near IR region. The presence of the functional groups such as O–H, C–H, C–O, C=O in the grown crystals was confirmed by FT-IR analysis. CHN analysis was carried out to confirm the presence of L-threonine in the grown crystals. Microhardness study on the crystals revealed that the hardness number H_v increased with the applied load. The growth pattern of the crystals were analyzed through etching analysis from which the etch patterns in the shape of 'step-triangle' were observed. The second harmonic generation (SHG) properties of pure and L-threonine doped tartaric acid crystals were confirmed by Kurtz-Perry powder technique.

Keywords: *crystal growth; optical materials; growth from solutions; X-ray diffraction*

1. Introduction

Generation of coherent blue light through the process of second harmonic generation (SHG) from near infrared (NIR) laser sources is an important technological challenge that has attracted researchers' attention because of its importance in providing key functions of frequency shifting, optical modulation, optical switching, optical logic and optical memory for the emerging technologies in the areas such as telecommunication, signal processing and optical interconnections [1].

Nowadays, many researchers are interested in studying nonlinear optical (NLO) properties of organic molecules and polymers. These materials are widely investigated due to their high nonlinear optical properties, rapid response in electro-optic effects and large second or third-order hyperpolarizabilities compared to inorganic NLO materials [2]. Major challenges with organic NLO crystalline materials are the difficulty in growing larger sized single crystals with optically superior qualities. Also, their fragile nature makes them difficult to process after growth [3].

L-tartaric acid and basic compounds form an important class of materials as they exhibit interesting electrical and optical properties. Some crystals of this family are ferroelectric (lithium thallium tartrate, calcium tartrate) [4]; some others are piezoelectric (lithium ammonium tartrate) [5] and some of these compounds show second harmonic generation efficiency higher than urea (cobalt tartrate, holmium tartrate). Examples of such systems are urea-tartaric acid [6]; cobalt tartrate [7]; holmium tartrate [8]; calcium tartrate [9]; cadmium tartrate [10], etc. L-tartaric acid ($C_4H_6O_6$) (TA) has higher laser damage threshold value (5.4 GW/cm^2), which is one of the essential properties for its utilization in devices involving laser, but the SHG efficiency of L-tartaric acid was

*E-mail: rarunpsgtech@yahoo.com

reported to be 0.88 times of that of standard KDP crystal [11]. For the mentioned reasons, the present research work is focused on the enhancement of SHG efficiency of TA single crystals by adding suitable dopants.

Amino acids contain a large number of optically active atoms which show highly efficient second-harmonic generation (SHG) efficiency and are promising candidates for coherent blue-green laser generation and frequency doubling applications [12]. Moreover, amino acids, like L-alanine, L-histidine, and L-threonine ($C_4H_9NO_3$), have special features, such as (i) molecular chirality, (ii) wide transparency in the visible and UV ranges, and (iii) zwitterionic character. The molecular chirality nature of material forces the molecule to crystallize in a noncentrosymmetric space group, which is an essential criterion for an SHG material. The zwitterionic character paved way for achieving superior properties such as high electro-optic parameters and improved mechanical and thermal strengths [13]. Among these compounds, L-threonine is an important amino acid which has SHG efficiency higher than that of many amino acids and their crystal family [14]. L-threonine (LT) with the molecular formula $C_4H_9NO_3$ is an uncharged polar amino acid that crystallizes in the noncentrosymmetric space group $P2_12_12_1$. LT exhibits orthorhombic structure with the unit cell parameters a = 13.611 Å, b = 7.738 Å and c = 5.144 Å [15]. It contains two asymmetric carbon atoms with a single carboxylate (COO^-) and amino (NH_3^+) groups.

Single crystals of pure and LT doped tartaric acid (LT/TA) were grown in the present work and were subjected to the following characterization studies: powder XRD, UV-Vis-NIR absorption and transmission spectra, FT-IR analysis, CHN analysis, microhardness, etching analysis and NLO test. The crystal growth and the performed characterization have been presented and discussed.

2. Crystal growth

Organic nonlinear optical (NLO) single crystals of pure and L-threonine added tartaric acid (LT/TA) were grown by slow evaporation technique using deionized water as a solvent at ambient temperature. Saturated solutions of pure TA and of 1 mol%, 3 mol% and 5 mol% L-threonine doped tartaric acid were prepared by dissolving them in double distilled water in separate beakers. The solutions were stirred well using a temperature controlled magnetic stirrer to get a homogeneous mixture of the solutions. Saturated solutions of pure and LT/TA were allowed for slow evaporation to enable the growth of pure and LT/TA single crystals. Finally, the saturated solutions were kept in an undisturbed environment at room temperature.

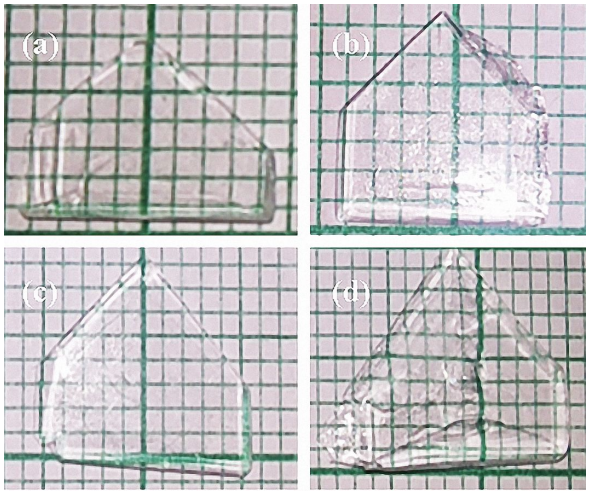

Fig. 1. Photographs of (a) pure TA, (b) 1 mol%, (c) 3 mol%, (d) 5 mol% L-threonine doped tartaric acid single crystals.

Good quality crystals with triangular shapes were harvested in a period of 25 to 30 days with the dimensions of 8 mm × 6 mm × 5 mm, 7 mm × 7 mm × 6 mm, 10 mm × 8 mm × 6 mm and 13 mm × 10 mm × 5 mm for pure, 1 mol%, 3 mol% and 5 mol% LT doped TA, respectively. The photographs of the grown crystals are shown in Fig. 1.

3. Results and discussion

3.1. Powder X-ray diffraction analysis

Powder X-ray diffraction patterns of pure, L-threonine doped tartaric acid single crystals were recorded at room temperature using Rigaku

X-ray diffractometer operating with CuKα radiation (λ = 1.540 Å). Recording was performed with the scan speed of 10°/min. The X-ray diffraction was recorded by a continuous scan in 2θ/θ mode from 10° to 70°. The recorded powder XRD pattern is shown in Fig. 2. Lattice parameter values of the grown crystals were calculated and are listed in Table 1.

From this analysis, it is confirmed that the grown crystals exhibit monoclinic crystal structure. The results were compared with the available JCPDS Card No. 33-1883. The peaks obtained from the grown crystals match well with the JCPDS data. The slight variation in the lattice parameters and the cell volume for the doped crystals can be attributed to the accommodation of L-threonine in the grown crystals. Sharp and well-defined peaks confirm the superior crystallinity of the grown crystals.

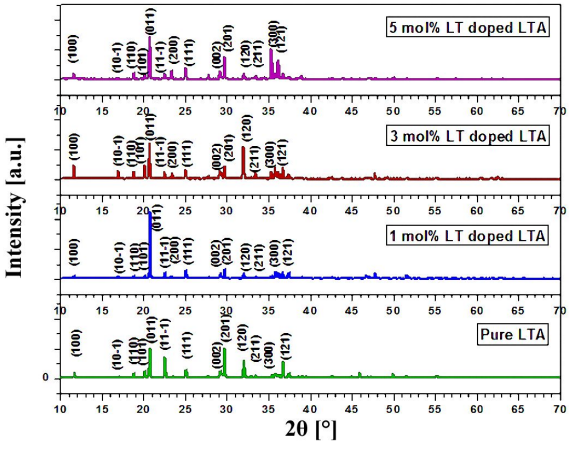

Fig. 2. Powder XRD pattern of pure and L-threonine doped tartaric acid crystals.

3.2. UV-Vis-NIR analysis

The UV-Vis-NIR absorption and transmittance spectral analysis of pure and doped single crystals with 1 mm thickness was carried out using UV-Vis-NIR spectrophotometer in the wavelength range of 200 nm to 1200 nm and the results are shown in Fig. 3. The transmittance spectra show that there is an improvement in the transmittance percentage from ≈68 % to ≈96 % caused by the addition of the dopant. No characteristic absorption has been found in the wavelength ranging from 285 nm to 1200 nm. The UV transparency lower cutoff wavelength of pure and L-threonine doped tartaric acid single crystals occurs around 281 nm. As there is no absorption in the entire visible region, LT/TA can be used as a potential material for second harmonic generation in the visible region.

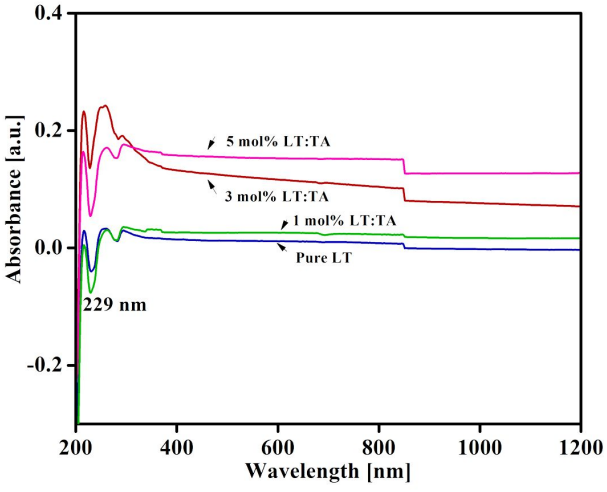

(a)

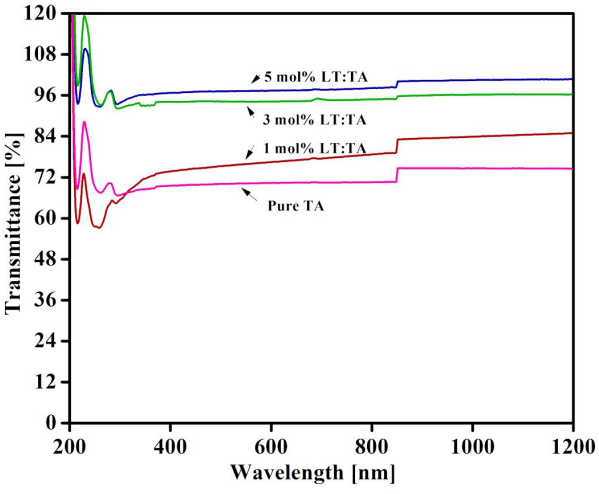

(b)

Fig. 3. (a) Absorption curve of pure and LT doped TA single crystals; (b) transmittance curves of pure and doped single crystals.

The dependence of optical absorption coefficient on photon energy helps to study the band structure and the type of transition

Table 1. Lattice parameter values of the grown crystals.

Sample	Lattice parameters			Cell volume	β	$\alpha = \gamma$
	a [Å]	b [Å]	c [Å]	[Å^3]	[°]	[°]
Pure TA	7.59	6.00	6.17	280.98	98.90	90
1 mol% LT doped TA	7.65	6.02	6.18	284.60	99.39	90
3 mol% LT doped TA	7.65	6.04	6.19	286.01	99.40	90
5 mol% LT doped TA	7.73	5.99	6.20	287.07	100.11	90

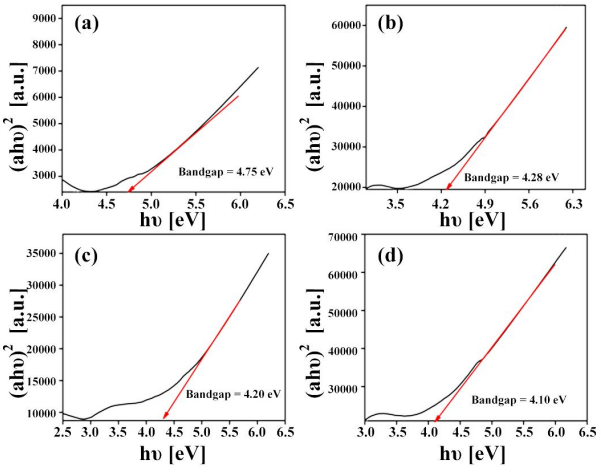

Fig. 4. Plot of $(\alpha h\upsilon)^2$ vs. hυ of (a) pure TA, (b) 1 mol%, (c) 3 mol%, (d) 5 mol% doped single crystals.

of electrons [16]. The optical absorption coefficient α can be calculated from the transmittance using the following relation:

$$\alpha = \frac{2.3036 \log[1/T]}{d} \tag{1}$$

where T is the transmittance and d is the thickness of the crystal. Several wide band gap materials possess excellent transmittance properties in the visible region. The energy dependence of the absorption coefficient provides information on the type of band gap. Similar to an indirect band gap semiconductor, the crystal under study has an absorption coefficient obeying the following relation for high photon energies hυ:

$$(\alpha h\nu)^{1/2} = A(E_g - h\nu) \tag{2}$$

where E_g is the optical band gap of the crystal, and A is a constant. The variations of $(\alpha h\upsilon)^2$ versus hυ in the fundamental absorption region are plotted in Fig. 4. E_g can be evaluated by extrapolation of the linear part of the plot [17]. The optical band gap is found to be 4.75 eV, 4.28 eV, 4.20 eV and 4.10 eV for pure, 1 mol%, 3 mol% and 5 mol% LT doped TA, respectively.

3.3. FT-IR analysis

Fourier transform infrared (FT-IR) analysis was carried out to identify the functional groups present in the grown crystals of pure, 1 mol%, 3 mol% and 5 mol% LT doped tartaric acid single crystals. The spectrum was recorded using a Shimadzu FT-IR-8400S spectrometer adopting KBr pellet technique in the range from 400 cm^{-1} to 4000 cm^{-1} and is shown in Fig. 5.

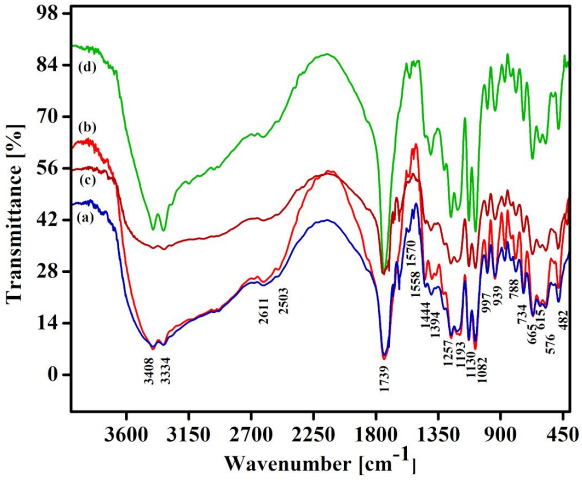

Fig. 5. FT-IR spectra of (a) pure TA, (b) 1 mol%, (c) 3 mol%, (d) 5 mol% L-threonine doped tartaric acid single crystals.

As the L-tartaric acid molecule does not have any symmetry [18], the internal vibrations of L-tartaric acid may be classified as those arising

from O–H, C–H, C–O, C=O groups. A strong but broad peak around 3408 cm^{-1} is due to the presence of O–H stretching in the carboxyl group. The very strong peaks observed at 1739 cm^{-1} and 1741 cm^{-1} indicate the presence of C=O stretching. The weak peaks at 1440 cm^{-1}, 1442 cm^{-1} and 1446 cm^{-1} are due to the combination of C–O stretching and O–H deformation. The characteristic absorption and bonding assignments of the functional groups are listed in Table 2. The FT-IR analysis confirms the presence of functional groups in the grown crystals.

3.4. CHN analysis

The chemical compositions of the grown crystals were determined by using CHN analysis for the pure and TA doped crystals. The CHN analyses were performed by Elementar Model Vario EL III using helium as a carrier gas. The percentage of carbon, hydrogen and nitrogen is given in Table 3.

The results confirm that the compositions of the grown pure TA crystals are in good agreement with the expected compositions (theoretical calculation). The presence of nitrogen is observed only in the LT-doped TA crystals and it is found to increase with the dopant concentration. This clearly indicates the incorporation of the dopant in the crystal lattice.

3.5. Microhardness test

Hardness of a material is the measure of resistance it offers to plastic deformation. The hardness of the material plays a significant role in device fabrication. Hardness of a crystal carries information about the crystal structure, yield strength and molecular bindings of the material. Microhardness study is undertaken to understand the plasticity of a substance [19].

For a static indentation test, the load was varied from 25 to 100 g and the time of indentation was maintained constant at 10 seconds for all the trials. By using a micrometer eyepiece, the diagonal lengths of indented impressions obtained for various loads were measured. The Vickers hardness number (H_v) is defined as the test force divided

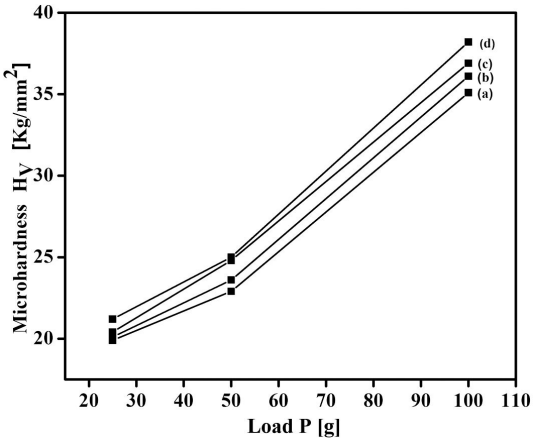

Fig. 6. Microhardness studies on (a) pure TA, (b) 1 mol%, (c) 3 mol%, (d) 5 mol% L-threonine doped tartaric acid single crystals.

by the actual area of the residual indent which is calculated using the following relation [20]:

$$H_v = \frac{2P}{d^2}\sin\frac{136}{2} = \frac{1.8544 \times P}{d^2}(kg/mm^2) \quad (3)$$

where the mean diagonal is $d = (d_1 + d_2)/2$ and its units are in millimeter (mm), and P is the applied load expressed in kilogram (kg). A graph has been plotted between hardness number H_v and applied load P for pure TA and of 1 mol%, 3 mol%, 5 mol% L-threonine doped tartaric acid crystals as shown in Fig. 6. The hardness increases gradually with the increase in load and above 100 g, cracks are developed on the smooth surface of the crystals due to the release of internal stresses generated locally due to indentation. Hence, it may be suggested that the LT/TA crystals may be used for the device fabrication below the applied load of 100 g.

The Meyer index number was calculated from the Meyer law, which relates the load and indentation diagonal length by the relation $P = k \cdot d^n$, where k is material constant and n is the Meyer index. In order to calculate the value of n, a graph has been plotted for log d versus logP as shown in Fig. 7. The graph is a straight line; the slope of this straight line gives the value of n. The calculated value of n was found to be 1.57, 1.54, 1.50 and 1.46 for pure, 1 mol%, 3 mol% and 5 mol% LT doped TA, respectively. According to the literature [21], the value of n lies between 1 to 1.6 for harder materials

Table 2. Characteristic absorption and bond assignments of pure and L-threonine doped tartaric acid single crystals.

Wavenumber [cm^{-1}]				
Pure LA	1 mol% LT doped TA	3 mol% LT doped TA	5 mol% LT doped TA	Frequency assignments
3408, 3344	3406, 3329	3408, 3332	3404, 3329	O–H stretching of carboxyl group
2681, 2611	2681, 2611	2675, 2613	2679, 2609	Associated OH stretching
1739	1739	1741	1739	C=O stretching of tartaric acid
–	1625	1627	1627	Asymmetric bending of NH_3
1444	1440	1442	1440	Combination of C–H and O–H deformation
1311	1305	1305	1303	N=N–O symmetric stretching
1257, 1213	1257, 1213	1257, 1209	1257, 1211	C–O–C antisymmetric stretching
1130, 1082	1128, 1082	1128, 1082	1128, 1082	C–O stretching
997, 939	995, 939	995, 939	995, 939	Wagging of CH_2
867, 819, 790	869, 823, 788	869, 825, 788	871, 823, 788	CH out-of-plan deformation
734	734	734	734	COO^- scissoring mode
665, 615, 576	667, 615, 574	669, 615, 574	669, 613, 572	Wagging vibration of COO^-

Table 3. Percentage of carbon, hydrogen and nitrogen in pure and LT-doped TA crystals.

Crystal	C [%]	H [%]	N [%] [%]
Pure TA (Calculated)	32.01	4.02	-
Pure TA (Observed)	32.09	4.11	-
1 mol% LT doped TA	34.61	5.54	4.90
3 mol% LT doped TA	34.65	5.78	4.99
5 mol% LT doped TA	34.69	5.97	5.20

and above 1.6 for softer materials. Hence, it may be concluded that the grown crystals belong to the category of hard materials.

3.6. Etching studies

Etching is a very common and inexpensive technique to reveal dislocations and lattice inhomogeneities present in the grown crystals. Patterns observed on surfaces such as spirals, rectangles, hillocks and step-patterns, etc, yield considerable information on the growth process and growth mechanism of a crystal [22]. Well-defined etch patterns were obtained at the dislocation sites when the surface was etched.

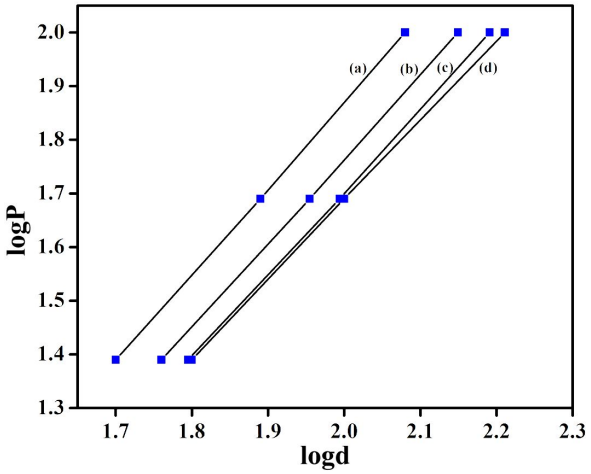

Fig. 7. Plot of logP vs. logd for (a) pure TA, (b) 1 mol%, (c) 3 mol%, (d) 5 mol% L-threonine doped tartaric acid single crystals.

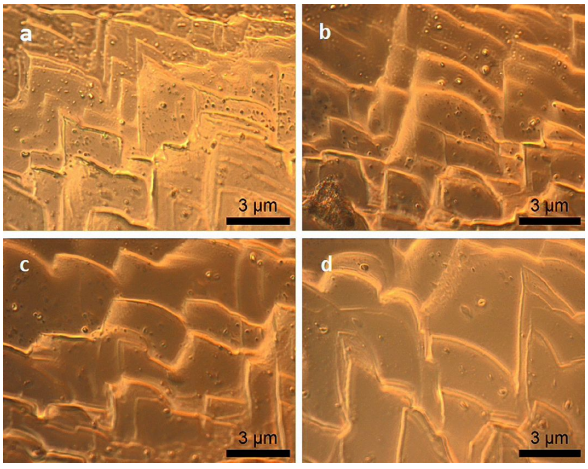

Fig. 9. Etch pit pattern of 3 mol% LT doped TA crystal with different etching times (10 s, 20 s, 30 s and 40 s shown in (a), (b), (c) and (d), respectively).

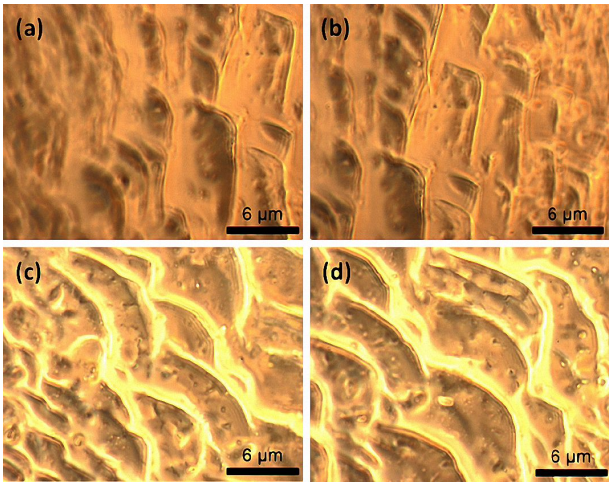

Fig. 8. Etch pit patterns of (a) pure TA, (b) 1 mol%, (c) 3 mol%, (d) 5 mol% LT doped TA single crystals for etching time of 10 s.

Chemical etching studies were carried out on the as-grown crystals of pure and LT doped TA single crystals to investigate the distribution of structural defects. The surfaces of the samples were polished and then etched using deionized water as an etchant at room temperature for varying etching times (10 s, 20 s, 30 s and 40 s). Then, the samples were soaked with a filter paper and examined under an optical microscope in reflection mode. Fig. 8 illustrates the typical etch patterns observed on the surface of pure TA, 1 mol%, 3 mol%, 5 mol% LT doped TA single crystal when they were etched with deionized water for 10 s.

Fig. 9 illustrates the typical etch patterns observed on the 3 mol% LT doped TA crystal for varying etching times. When the crystals were etched in water, the triangular type etch pits were observed. In Fig. 9, several etch pits with identical shape can be identified. By increasing the etching time, the pattern remains the same but the size of the etch pits is found to increase. Dislocations are formed due to inclusions in the grown crystals. The formation of inclusions destroys the normal building up of lattices, which results in stress and lattice mismatch in the grown crystals [23]. In order to relax the stress and reduce the lattice mismatch, lots of dislocations are produced. That is why so many dislocation etch pits are observed in the doped TA crystals.

3.7. Powder SHG test

To find the SHG conversion efficiency of the NLO crystals, powder technique developed by Kurtz and Perry was used. However, the SHG efficiency observed for a given sample may vary due to a number of parameters, including laser wavelength, particle size, temperature, crystallization solvent and other parameters involved

in sample preparation. In the present investigation, pure and LT doped TA crystals were ground into fine powders (average particle size were around 3 μm) and packed in microtubes mounted in the path of laser pulses from a Nd:YAG laser with the operating wavelength of 1064 nm with a pulse width of 6 ns and repetition rate of 10 Hz. The input energy was 0.68 mJ per pulse. The second harmonic generation of the grown crystals was confirmed by a green emission with the wavelength of 532 nm from the samples. SHG signals of 350 mV and 483 mV were obtained from pure TA and 5 mol% LT doped TA crystallites, respectively. The second harmonic generation efficiency of 5 mol% LT doped TA crystal was found to be 1.38 times of that of pure TA crystal.

4. Conclusions

Good quality nonlinear optical (NLO) single crystals of pure tartaric acid and L-threonine doped tartaric acid (LT/TA) were grown by slow evaporation technique at room temperature. Powder XRD analysis revealed that the grown crystals belong to a monoclinic crystal system. The optical absorbance spectrum revealed that the crystal has a wide optical window from 285 nm to 1200 nm which is very important for materials possessing nonlinear optical properties. The UV cut-off wavelength for the grown crystal was found to be 281 nm and the optical band gap was established as 4.75 eV, 4.28 eV, 4.20 eV and 4.10 eV for pure, 1 mol%, 3 mol% and 5 mol% LT doped TA, respectively. The characteristic absorption and bonding assignments of the functional groups were confirmed using FT-IR spectroscopy. The presence of dopant in the crystal lattice was confirmed by CHN analysis. Mechanical behavior of the grown crystals was investigated by microhardness study and it was found that the grown crystals belong to hard materials category. From the etching studies, well-defined step triangular etch pits were observed on the surface of the grown crystals. The second harmonic generation efficiency of 5 mol% LT doped TA crystal was found to be 1.38 times of that of pure TA crystal. Hence, the enhancement of the second harmonic generation efficiency of TA crystals due to the incorporation of the dopant L-threonine was confirmed.

References

[1] MARTIN BRITTO DHASS A., SURESH M., BHAGAVANNARAYANA G., NATARAJAN S., *J. Cryst. Growth*, 309 (2007), 48.

[2] MARY LINET J., JEROME DAS S., *Mater. Chem. Phys.*, 126 (2011), 886.

[3] MOOLYA B.N., DHARMAPRAKASH S.M., *J. Cryst. Growth*, 290 (2006), 498.

[4] GON H.B., *J. Cryst. Growth*, 102(1990), 501.

[5] IVANOV N.R., *Ferroelectrics Lett.*, 2 (1984), 45.

[6] MENG F.Q., LU M.K., CHEN J., ZHANG S.J., ZENG H., *Solid State Commun.*, 101 (1997), 925.

[7] GU Y., YANG M., *Cryst. Res. Technol.*, 43 (2008), 1331.

[8] WANT B., AHMAD F., KOTRU P.N., *J. Cryst. Growth*, 299 (2007), 336.

[9] PAREKH B.B., JOSHI V.S., PAWAR V., THAKER V.S., JOSHI M.J., *Cryst. Res. Technol.*, 44 (2009), 31.

[10] ARORA S., KKOTHARI A., AMIN B., CHUDASAMA B., *Cryst. Res. Technol.*, 42 (2007), 589.

[11] BHAT M.N., DHARMAPRAKASH S.M., *J. Cryst. Growth*, 243 (2002), 526.

[12] KAJZAR F., MESSIER J., CHEML A., ZYSS D.S., *J. Nonlinear Optical Properties of Organic Molecules and Crystals*, Academic Press, New York. 1987, 51.

[13] RAZZETTI C., ARDOINO M., ZANOTTI L., ZHA M., PAORICI C., *Cryst. Res. Technol.*, 37 (2002), 456.

[14] JAIKUMAR D., KALAINATHAN S., *Cryst. Res. Technol.*, 43 (2008), 565.

[15] SHOEMAKER D.P., DONOHUE J., SCHOMAKER V., COREY R.B., *J. Am. Chem. Soc.*, 72 (1950), 2328.

[16] TIGAU N., RUSU G.I., CIUPINA V., PRODAN G., VASILE E., *J. Optoelectron. Adv. M.*, 7 (2005), 727.

[17] CHAWLA A.K., KAUR D., CHANDRA R., *Opt. Mater.*, 29 (2007), 995.

[18] SENTHIL MURUGAN G., RAMASAMY P., *AIP Conf. Proc.*, 1447 (2012), 511.

[19] SOMASUNDARI C.V., *Arch. Phys. Res.*, 3 (2012), 283.

[20] MOTT B.W., *Micro-Indentation Hardness Testing Bulterworths*, London, 1956, 206.

[21] LAL B., BAMZAI K.K., KOTRU P.N., WANKLYN B.M., *Mat. Chem. Phys.*, 85 (2004), 353.

[22] SANGWAL K., HEIMANN R.B., *Etching of Crystals: Theory, Experiments and Applications*, North Holland, Amsterdam, 1987.

[23] SANGWAL K., OWCZAREK I., *J. Cryst. Growth*, 129 (1993), 640.

Received 2017-07-17
Accepted 2018-10-13